PORT SAID ENGINEERING RESEARCH JOURNAL
Faculty of Engineering - Port Said University
Volume 26 No. 2 pp: 102:111

Weldability of Dissimilar Aluminum Alloys AA7075-AA5083 Using FSW Technique

H. Abd El-Hafez[1, *]

[1] *Production Engineering and Mechanical Design Department, Faculty of Engineering, Port Said University, Port Said, Egypt, email: abdelhafez1@eng.psu.edu.eg*

*Corresponding author, *abdelhafez1@eng.psu.edu.eg*, DOI: 10.21608/PSERJ.2021.94331.1140 (doi.org)

Received 5-9-2021,
Revised 14-10-2021,
Accepted 24-10-2021

ABSTRACT

The influence of the friction stir welding conditions on weldability of two very popular aluminum alloys, in welding construction, is analyzed in this study. Non-heat-treatable (AA5083-H111) and a heat-treatable aluminum (AA7075-T651) alloy, are characterized by markedly different strengthening mechanisms and microstructural evolution at increasing temperatures. Dissimilar weldments were produced by the friction stir welding process under different welding conditions. The welding parameters were rotational speed, welding speed, tool geometry و material location and tool position. Their metallographic and mechanical properties were analyzed and compared using metallographic examination, hardness test and tensile test.

Dissimilar joints show some defects that differ due to the welding conditions. Higher rotational and welding combination speeds achieve sound joint associated with higher strength compared to the other welding joints. Moreover, when the soft material is located at the retreating side the weldment performance is improved.

Due to the relationship between metal formability and temperature, the heat distribution under various welding parameters was studied. The temperature analysis indicates that increasing the rotational speed increases the produced heat and consequently, the mixing efficiency of the welded alloys.

Keywords: Friction stir welding, Dissimilar aluminum alloys, Welding parameters, Mechanical properties, Welding tool geometry.

1. INTRODUCTION

Friction Stir Welding (FSW) offers immense benefits over traditional welding attributable to the absence of melting and a small energy requirement. Accordingly, the quality of the weldment is improved [1].

The joining of dissimilar materials by any welding process usually is difficult due to the many variations in metallurgical and mechanical properties. The joints of dissimilar materials are becoming more employed in several industries because of its technological and cost-effective advantages [2].

Ahmed et al. [3] studied the metallographic behavior for similar and dissimilar two aluminum alloys (AA5083 and AA7075) friction stir weldments. They observed that the crystallographic texture in the nugget zone revealed a simple shear texture without a significant influence of varying the welding speed. The dissimilar joints exhibited performance ranged between 77 and 87% relative to the strength of AA5083 base metal. Moreover, Yoon et al. [4] concluded that the grain size in the stir zone (SZ) was smaller than that of the base metal and was decreased with the decrease of the tool rotation speed and with the increase of the tool traverse speed.

Parameters such as travel speed, tool geometry, joint thickness, and material composition are the influence parameters that control the mechanical properties of FSW weldments [5,6]. mechanical properties (particularly tensile strength) of joints [5].

A suitable combination of the tool rotational and traverse speeds is very important for obtaining defect free joints of FSW [7]. Several defects are occurred during FSW process due to the lack of unappropriate material flow, and these defects depended on numerous factors [5,8]. However, the tunnel defect was detected on the advanced side (AS) near the bottom surface. The tunnel defect has been attributed to the extra heat input and plastic flow under the inappropriate FSW conditions [4,5]. Therefore, Shojaeefard et al. [7] concluded that higher strength is achieved for friction stirred the dissimilar AA5083-O/AA7075-O at 1400 rpm and 20 mm/min.

Luo et al. [9] found, analytically, that when the rotational speed to welding speed ratio increased, the temperature distribution, around the pin, tended to transform from non-uniform to uniform.

Also, Aziz et al. [10] proved that low rotational speed cause lacking temperature distribution through low frictional and plastic dissipation energy which ultimately results weld defects. Increasing the weld and rotational speeds, the influence of plastic dissipation energy increases leading to improve the weld quality. Furthermore, increasing the (ω) increases the heat input due to the tool shoulder generate about 90% of frictional heat [11]. While the heat input decreases at increasing the welding speed [11], causes insufficient plastic flow of material producing the defects [6]. Moreover, Yu et al. [12] demonstrated that the tensile stress increases with decreasing the welding speed. However, larger tensile stress appears under the tool shoulder with increasing the rotational speed.

Previous studies [13,14] proved that the effect of pin/shoulder diameter ratio (D/d) has minor influence on increasing temperature, more frictional heat is produced by increasing the shoulder diameter leading to increase in material softening and consequently improving in material flow [13]. According to Saravanan et al. [15], at higher D/d ratios, excessive heat generation could be softening the weld zone therefore a turbulent flow between two welded materials can be generated. Due to the inadequate mixing of materials, the defect nucleation in the weld zone becomes more.

Kishore et al. [16] concluded that the lowest temperature is produced on softer material side with change in position of materials since excess heat is generated on harder material side because of viscous dissipation. Also, the mixing efficiency depends on location of material on the retreating and advancing side. Moreover, Cole et al. [17] and Gerard [18] proposed that the harder material have to be on the advancing side to eliminate the internal defects.

Furthermore, the pulsating action caused by the flats on the tool pin sides (for non-circular pins) results in thoroughly microstructure across the weldments and relatively increase the peak temperature. This behaviour results in improved regularity in hardness profiles in the event of tool pins with a growing number of flats [19].

Many researchers proved that the influence of tool design on the joint performance. Abd El-Hafez & El-Megharbel [20] investigated the friction stir welding of dissimilar aluminum alloys AA 2024- and AA 5083-H111 and concluded that square pin improves the joint strength compared to prism and stepped geometries due to the four pulses per revolution. Moreover, Waheed et al. [21] stated that the generated heat increases from the square pin to hexagonal one but then reduces to the triangular pin profile.

From the previous studies, this work aims to find the suitable welding parameters to fabricate the sound dissimilar FS-weldment of aluminum alloys AA7075-T651 and AA5083-H111.

2. EXPERIMENTAL WORK

To evaluate the effect of welding conditions, an experimental program was designed, Table 3. Friction stir (FS)-weldments were carried out at different welding speeds on vertical milling machine using a special fixture to ensure a proper arrangement of the specimens throughout the process, Fig. 1.

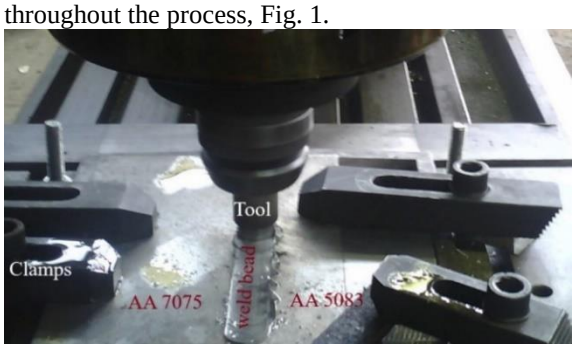

Fig. 1 Friction stir welding setup

2.1. Materials

Two aluminum alloys of 7075-T651 and 5083-H111 were used, in this study, to perform the dissimilar friction stir weldments.

The aluminum alloys were received in sheets with the required dimensions of 250x100x5 mm. Their chemical compositions and mechanical properties are listed in Table 1 and Table 2, respectively.

Table 1 The chemical compositions of Al-alloys.

Aluminum Alloy	Chemical composition, wt.%								
	Si	Fe	Cu	Mn	Mg	Cr	Zn	Ti	Al
5083 -H111	0.1344	0.3411	0.0282	0.4380	4.0838	0.0946	0.0389	0.0072	bal
7075-T651	0.4	0.5	1.7	0.3	2.5	0.2	5.5	0.15	bal

Table 2 The Mechanical properties of Al-alloys.

Material	**Mechanical properties**			
Al 5083 -H111	Tensile Strength MPa	Yield strength MPa	Elongation %	Hardness (HV)
	266.2	242.4	35.1	83
Al 7075-T651	553.1	553.1	10.7	175

2.2. Welding Tools

In this study, steel-H13 tools with 10º concave shoulder and different diameters of 15, 17.5 and 20 mm accompiened with 5 mm pin diameter and 4.7 hight were manufactured to form the shoulder/pin ratios (3, 3.5 and 4). Furthermore, the effect of three pin geometries, square, triangular and threaded taper, Fig. 2, is studied where is used to manufacturing the welding tools.

2.3. Welding Parameters

Various welding parameters were chosen due to the previous studies and the primary experiments. Three values of rotational speed (ω), as well as for welding speed (v) were used to manufacturing the FS-joints. Also, the material location (advanced and retreating side) and tool shifting were considered as welding parameters, Table 3.

(a) Square (b) Triangular (c) Tapper threaded

Fig. 2 Photographs of the welding tools

2.4. Tests

To evaluate the effect of the welding parameters on the FS-joints performance (η), tensile, microhardness and metallographic examination were applied.

The tensile test is performed at a universal testing machine (MTS 100KN). The tensile specimens were cut perpendicular the welding line and milled to the standard dimensions of ASTM-E08. Each result represented an arithmetic mean of three specimens, at least, for each joint.

Metallographic and microhardness specimens were ground up to 1200 mesh, polished with diamond paste down to 1μm and etched using killer's reagent. Visual inspection and Light optical microscope, with an image analyzing software, was used to reveal the macro- and micro-structural analysis.

The Vickers microhardness test was performed with 0.5 Kg/10 sec through the various zones of the weldment (SZ; TMAZ; HAZ, and the parent alloys).

2.5. Temperature Measurements

The temperature during welding was measured using thermal infrared-camera and infrared thermometer which could measure up to 1200°C with accuracy ±1%. The temperature is measured at tool/material surface interface through all welding process.

3. RESULTS AND DISCUSSION

All specimens were subjected to visual inspection and metallographic examination. For primary experiments, it was noticed that some joints had visual defects or micro defects depending on the welding parameters. However, most FS-joints were sound and defects free. Fig. 3 shows some of these welding defects including diverse types such as pinhole and grain boundary defects. The size and type of these defects could be attributed to lack of penetration caused from lacking material flow under the pin. This is due to the unsuited generated friction temperature which agrees with previous studies [4–6]. On the other hand, threaded taper joint has a visible tunnel defect due to slipping the material around the pin, Fig. 3-b.

Table 3 Welding Parameters

Rotational speed (ω) (rpm)	Welding speed (v) (mm/min)	shoulder/pin ratio (R)	Pin Geometry	Advanced side/ Retrating side (AS/RS)
1400	80	3, 3.5 and 4	Square	7075/5083
	16			
	80			
900	16			
	40			
	80			
1120	16			
	40			
	80			
1400	16			
	40			
	80			
	16	4	Taper threaded	
	40			
	80			
	16	4	Triangle	
	40			
	80			
	16	4	Square	5083/7075
	40			
	80			
	80	4		7075/5083 With shiffting 1mm toward 5083

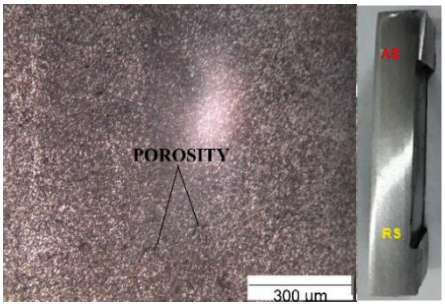

(a) square pin

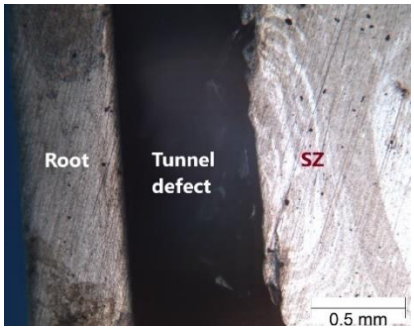

(b) threaded taper pin

Fig. 3 Stirred zone (SZ) with micro voids and

3.1. Microstructure Investigation

The metallographic examination shows differing in mixing behavior between specimens depends on the generated heat amount and tool geometry resulted a mixing efficiency.

3.1.1. Stir zone

The stir zone (SZ) is influenced by welding conditions which controlled the generated heat and the plastic deformation. The pin geometry effect is shown in Fig. 4(a, b) where both square and triangular achieved sound joints with different microstructures. The SZ microstructure shows different mixing behaviors where square one gave better homogeneity at the same welding conditions, Fig. 4. Also, under the shoulder, fine grains and good mixing were noticed, Fig. 5-a, compared to the SZ far away the shoulder, Fig. 5-b, where highest heat is generated.

3.1.2. Thermomechanical affected zone (TMAZ)

The microstructure of thermomechanical affected zone at both sides, advanced and retreating are shown in Fig.6. The advanced side is differing from retreating one. The deformed grains are flow in curves in direction of stirring at AS whereas it is not noticed at RS. However, the interface between SZ and TMAZ is quite sharp, Fig.6-a, whereas the stirred metal is diffused into parent metal at RS, Fig.6-b, which is proved also by other researchers [20,22,23].

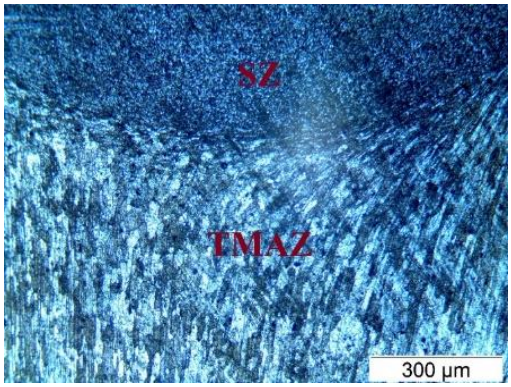

(a) Square

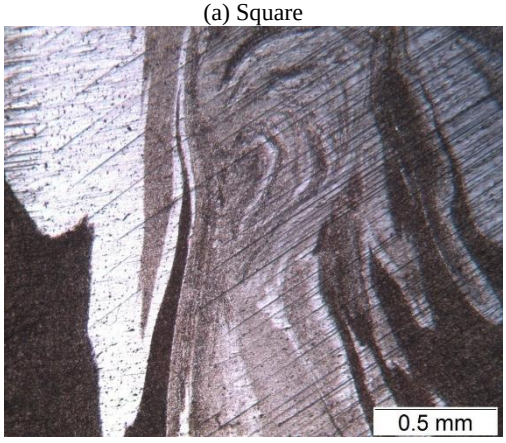

(b) Triangular

Fig. 4 Microstructure of stirred zone for dissimilar 7075/5083 joints performed using different pin geometries at 1400 rpm and 16 mm/min.

(a) fine grains and good efficiency

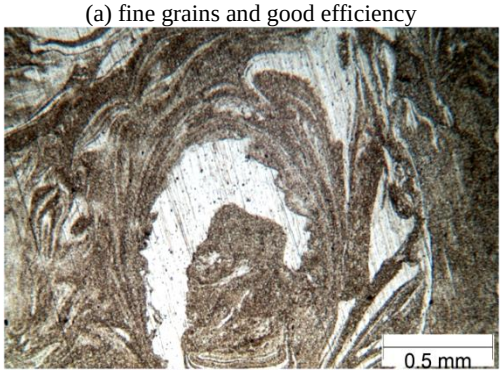

(b) Less efficiency

Fig. 5 The mixing efficiency in the stir zone

a) SZ/TMAZ interface at RS

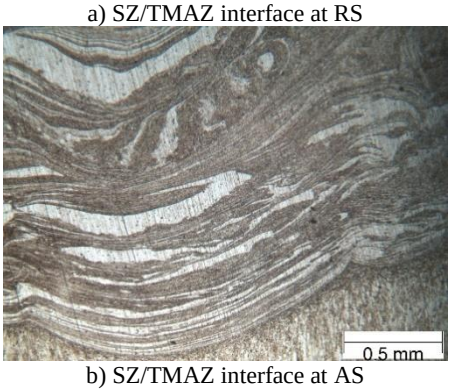

b) SZ/TMAZ interface at AS

Fig.6 Micrographs of TMAZ/SZ interference at advanced and retreating sides

3.2. The Generated Temperature

The temperature at tool shoulder/joint surface interface was recorded using infra thermal camera which is more accurate than infrared thermometer. Fig.7 shows thermal images and distribution charts for measuring temperature during FSW process at various welding parameters. The

examination was performed according to EN 13187 using a thermal imager. The average measuring readings, through the welding process, were plotted in Fig. 8Fig. 8. The results appeared a significant effect of rotational speed (ω) compared to welding speed (v) on the produced heat. The increase of (ω) increasing the temperature significantly, which is in good agreement with the previous studies [13,15]. However, at low temperature, there is a bad formability and consequently, poor mixing.

3.3. The Hardness Behavior

The Vickers microhardness tests were carried out through different regions of the weld. Figure Fig.9 shows the hardness profile throughout weldments for specimens that welded at 900 and 1400 rpm for various (**ν**). It could be identified three various zones through the specimen (SZ, TMAZ and base metal). The hardness variations could be attributed to the variation in microstructure, the homogeneity of the phases in the SZ and the mix behavior as mentioned by Salloomi et al. [24]. Specifically, the first region of AA 5083-base alloy can be clearly observed by the insignificant fluctuation of the hardness values. Though, obvious variant of the hardness values was achieved in TMAZ zone. Slight decrease of the hardness values has been found in SZ but less variation.

Though, the hardness has almost the same behavior for the whole specimens with noticeable difference in values. Variance from one specimen to another explains the effect of the welding conditions on issues like mixing performance, and grain size as stated by other studies [24,25].

3.4. Tensile Strength

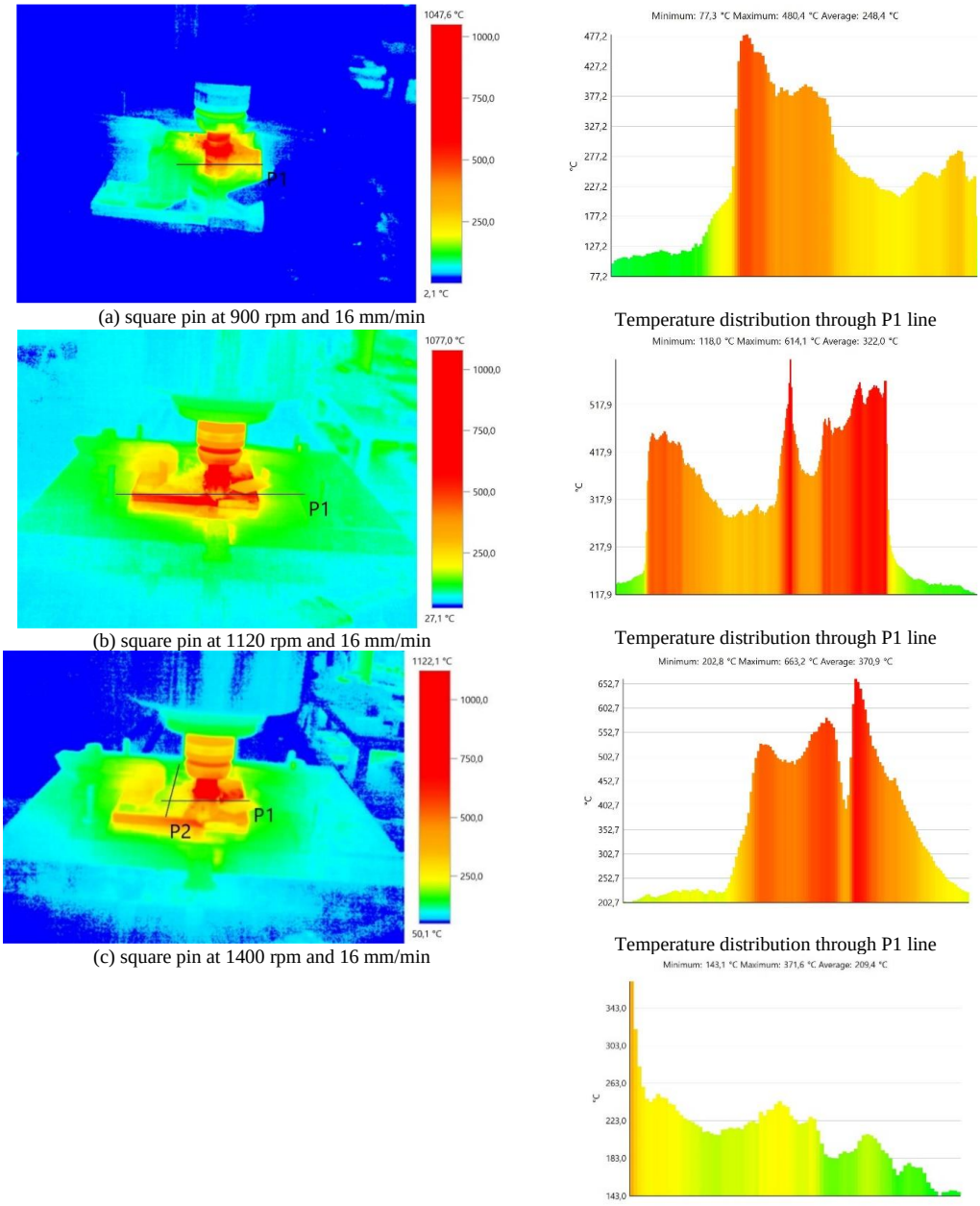

(a) square pin at 900 rpm and 16 mm/min

(b) square pin at 1120 rpm and 16 mm/min

(c) square pin at 1400 rpm and 16 mm/min

Fig.7 Thermal photographs and distribution charts for measuring temperature of FSW process at various welding parameters

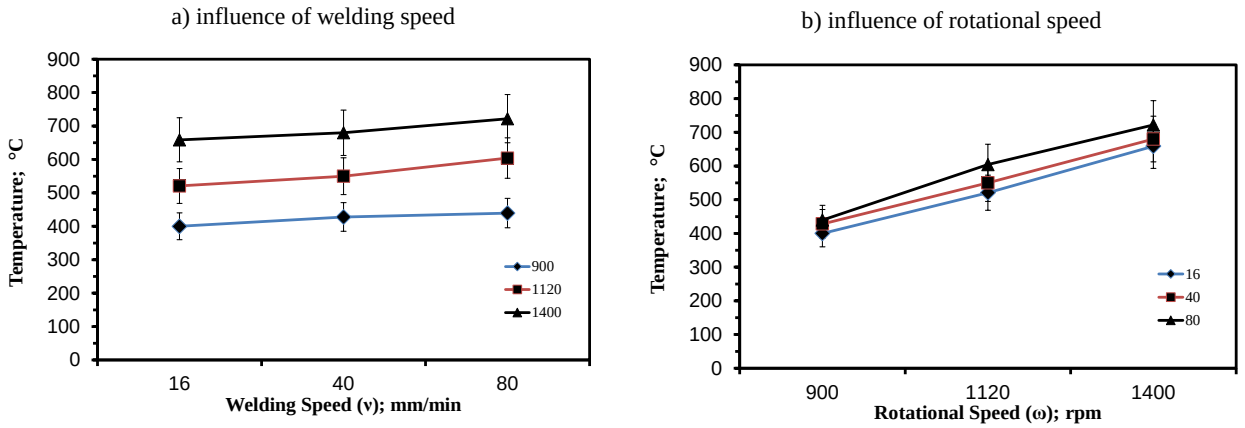

Fig. 8 Effect of welding speeds on the generated temperature using square tool pin.

All specimens have undergone tensile test to evaluate their mechanical properties. Three tensile specimens were presented one FS-joint and their arithmetic mean is plotted in the following figures. The tensile strength, as a function in joint performance (□), was discussed due to the welding conditions. The joint performance can be defined as the joint strength regarding the weakest base alloy, which is AA5083, in this study.

3.4.1. Effect of Tool Geometry

According to the metallographic examination, the threaded taper tool produced poor joints. Therefore, a comparison between triangular and square to evaluate the tool geometry effect on the joint performance. The results, Fig. 13, show that the square pin produces peak performance by the pulsed action that generating better stirring as a result of good metal flow. These findings agree well with previous studies [20,23,26]. Therefore, the welding conditions and tool shoulder effects are evaluated with square tool.

3.4.2. Effect of Material location

Higher strength and sound weldment are reached when harder alloy lies on AS, as previously mentioned [20,27–29]. Therefore, the effect of the material position is evaluated at 1400 rpm associated with various welding speed, Fig. 14. The material's location has significant impact joint's performance when the AA5083 lies at RS and the harder (AA7075) at the AS. This result is agreeing with previous studies [20,27–29] while disagree with Khodir & Shibayanagi [31]. Therefore, the welding parameters evaluation was done by locate AA7075 at the advanced side (AS).

3.4.3. Influence of Shoulder/Pin Ratio (R)

The shoulder/pin ratio (R) affect on the joint performance (η) at various welding speed (ν) was shown in Fig. 15 (a-c).

Fig. 15-a shows similar behaviour of η at 900 rpm (inverted bell). The R has insignificant variation between R=3 and R=4 except at **ν**=80mm/min where lower **η** at R=4. Lower **η** could be attributed to increasing the produced heat at surface with respect to weld root, faraway the shoulder.

In additions, at R=3.5, the **η** has lower values for various **ν**. At R=3, the good values could be related to the small bead and concentration heat around the pin. The higher performance at R=3 and **ν**=80 mm/min, is correlated to the tensile fracture in base metal (AA5083), Fig. 16-a, not in weld zone as the others, Fig. 16-b. The tensile specimens were fractured at SZ/TMAZ boundary due to localized softening as concluded by Ramanjaneyulu et al. [19].

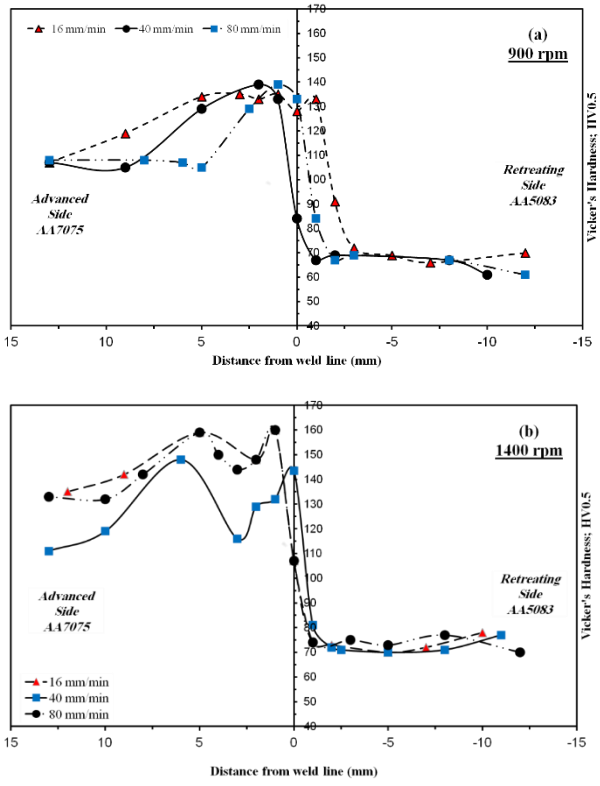

Fig.9 Influence of welding speed (ν) on the FS-weldments hardness at a steady rotational speed (□).

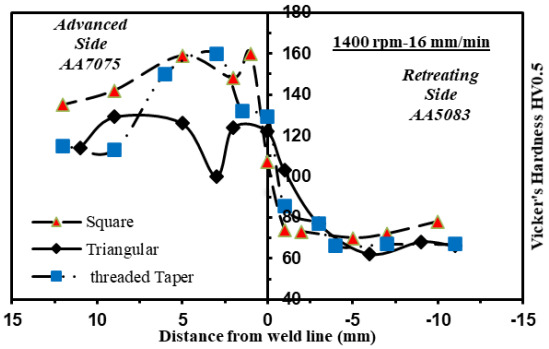

Fig. 10 Influence of pin form on the FS-weldment hardness.

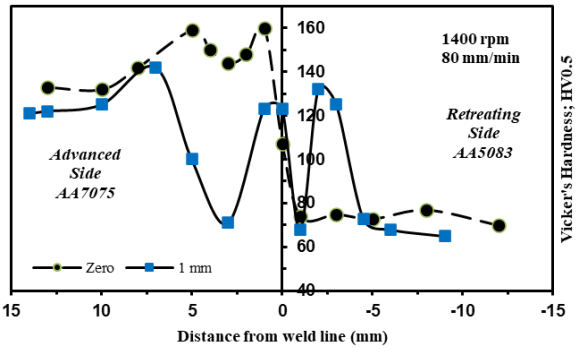

Fig. 11 Influence of tool shift, into AA5083, on the hardness of the FS-weldment.

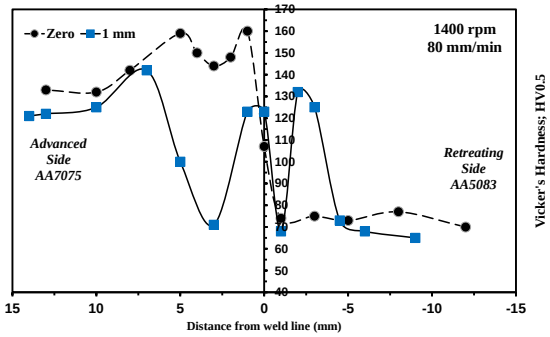

Fig. 12 Impact of number of welding sides on the joint hardness

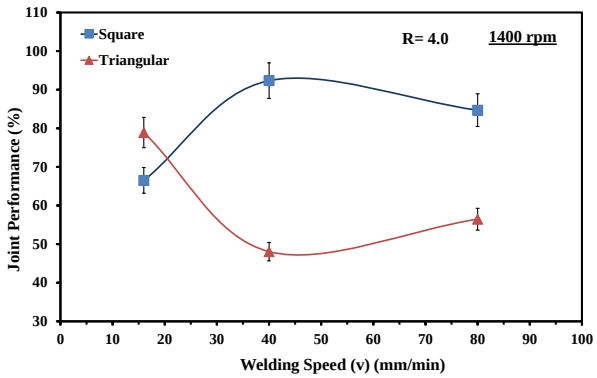

Fig. 13 Influence of tool geometry on the joint performance at various welding speeds

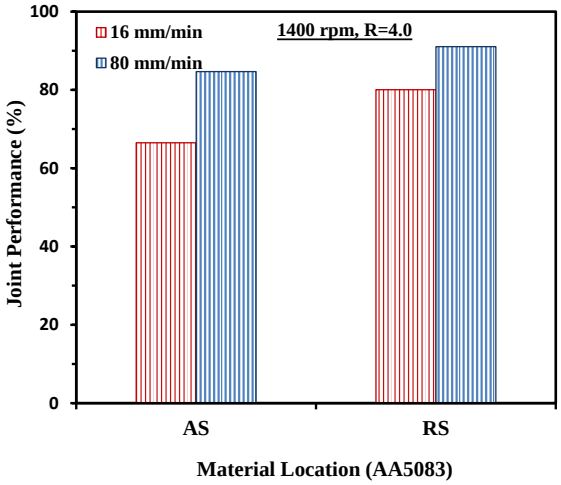

Fig. 14 Effect of AA5083 location (advanced or retreating) on the joint performance

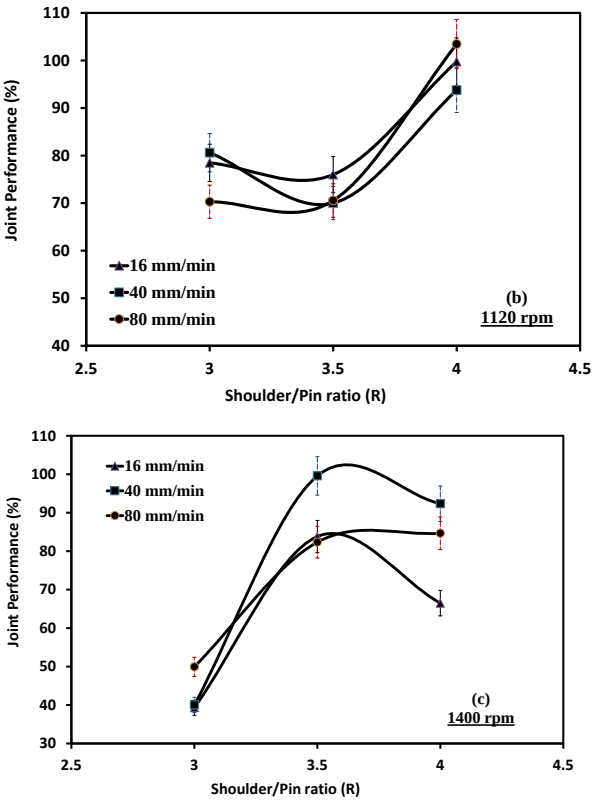

Fig. 15 Influence of shoulder/pin ratio on the joint performance at various welding speeds and constant rotational speed.

Moreover, at 1120 rpm shown in Fig. 15-b, best performance was noticed at R=4 for different **ν** that not increased than 100%. Also, neglected effect of **ν** is noticed.

The performance behaviour is changed at higher **ω**, Fig. 15-c, where the behaviour takes the bell shape. Lowest **η** is noticed at R=3 whereas the higher is at R=3.5 for **ν**=40

mm/min. This result achieved at 40 mm/min could be related to the suitable generated heat for formability of the stirred metal leading to good mixing without any micro defects as shown in Fig. 5. The variation in performance at various (**v**) could be impeached the micro voids presented in weld zone where the tensile fracture occurred. In addition, Finer dimples and uniform size particles can improve the strength and ductility as concluded by Guo et al. [31].

However, it can be concluded that the suitable producing heat depends on the proper combination of welding parameters (**v** and **ω**) and shoulder diameter as mentioned by previous studies [13,20,23,32].

(a) Fracture at AA5083

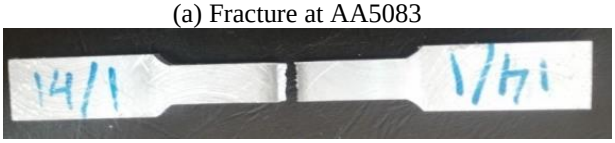

b) Fractured at stirred zone (weld line)

Fig. 16 Two types of tensile specimen fracture

3.4.4. Effect of tool shifting

To evaluate the effect of shifting toward the softness material (AA5083), the tool is shifted by 1 mm. The experimental results, Fig. 17, show an improvement for performance (**η**) which agree with conclusion of previous study [33].

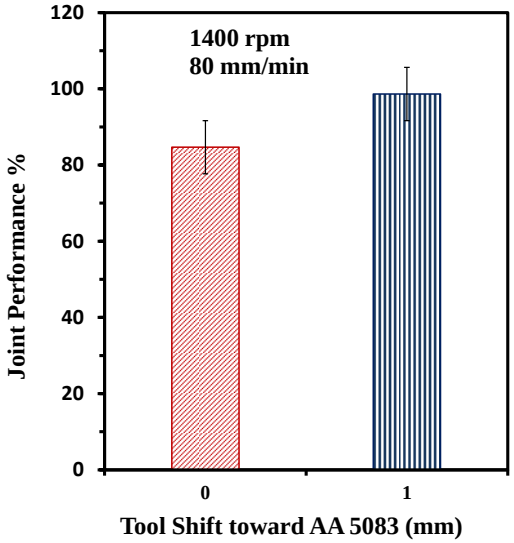

Fig. 17 Effect of tool shifting, for one mm, on the joint performance

4. CONCLUSIONS

From the results, it can be concluded the following.

1- Square tool pin achieves best strength due to good mixing effect.
2- The welding speed (***v***) has minor effect on the resulted temperature during FSW-process as well as the weldment performance.
3- The rotational speed has the major effect with respect to its influence on the produced friction heat.
4- Improving the mixing efficiency of welded materials improving the weldment strength as resulted at using the square pin associated the proper combination of diameters ratio (R) and rotational speed (ω).
5- The weldment hardness is not the first indicator of the sound joint due to the possibility of micro defects presence.
6- The soft material (AA5083) achieves better strength when it located at the retreating side (RS).
7- The shifting of the welding tool to soft material (AA5083), according to the weld line, plays an effective role in improvement of the mechanical properties.

ACKNOWLEDGMENT

The author would like to extend his thanks and gratitude to the technicians in the workshop of the Faculty of Engineering, Port Said University - Egypt. Grateful thanks to Mr. Mohamed Abdelhalim, the machine technician for his help to complete the experimental work.

Declaration of Competing Interest

The authors declare that they have no known competing financial interests or personal relationships that could have appeared to influence the work reported in this paper.

Conflicts of Interest

The author declares that there is no conflict of interest regarding the publication of this paper.

5. REFERANCES

[1] Quintana KJ, Silveira JLL. Mechanistic models and experimental analysis for the torque in FSW considering the tool geometry and the process velocities. Journal of Manufacturing Processes. 2017;30(October):406–17.

[2] Mehta KP, Badheka VJ. A review on dissimilar friction stir welding of copper to aluminum: Process, properties, and variants. Materials and Manufacturing Processes. 2016;31(3):233–54.

[3] Ahmed MMZ, Ataya S, El-Sayed Seleman MM, Ammar HR, Ahmed E. Friction stir welding of similar and dissimilar AA7075 and AA5083. Journal of Materials Processing Technology. 2017; 242:77–91.

[4] Yoon SO, Kang MS, Nam H Bin, Kwon YJ, Hong ST, Kim JC, et al. Friction stir butt welding of A5052-O aluminum alloy plates. Transactions of

Nonferrous Metals Society of China (English Edition). 2012;22(SUPPL.3):s619–23.
[5] Saeidi M, Manafi B, Besharati Givi MK, Faraji G. Mathematical modeling and optimization of friction stir welding process parameters in AA5083 and AA7075 aluminum alloy joints. Proceedings of the Institution of Mechanical Engineers, Part B: Journal of Engineering Manufacture. 2016;230(7):1284–94.
[6] Palanivel R, Laubscher RF, Vigneshwaran S, Dinaharan I. Prediction and optimization of the mechanical properties of dissimilar friction stir welding of aluminum alloys using design of experiments. Proceedings of the Institution of Mechanical Engineers, Part B: Journal of Engineering Manufacture. 2018;232(8):1384–94.
[7] Shojaeefard MH, Behnagh RA, Akbari M, Givi MKB, Farhani F. Modelling and pareto optimization of mechanical properties of friction stir welded AA7075/AA5083 butt joints using neural network and particle swarm algorithm. Materials and Design. 2013;44(January):190–8.
[8] Lertora E, Gambaro C. AA8090 Al-Li Alloy FSW parameters to minimize defects and increase fatigue life. International Journal of Material Forming. 2010;3(SUPPL. 1):1003–6.
[9] Luo J, Li S, Chen W, Xiang J, Wang H. Simulation of aluminum alloy flowing in friction stir welding with a multiphysics field model. International Journal of Advanced Manufacturing Technology. 2015;81(1–4):349–60.
[10] Aziz SB, Dewan MW, Huggett DJ, Wahab MA, Okeil AM, Liao TW. A fully coupled thermomechanical model of friction stir welding (FSW) and numerical studies on process parameters of lightweight aluminum alloy joints. Acta Metallurgica Sinica (English Letters). 2018;31(1):1–18.
[11] Waheed MA, Jayesimi LO, Ismail SO, Dairo OU. Modeling of heat generations for different tool profiles in friction stir welding: Study of tool geometry and contact conditions. Journal of Applied and Computational Mechanics. 2017;3(1):37–59.
[12] Yu H, Zheng B, Lai X. A modeling study of welding stress induced by friction stir welding. Journal of Materials Processing Technology. 2018;254(June 2017):213–20.
[13] Akbari M, Aliha MRM, Keshavarz SME, Bonyadi A. Effect of tool parameters on mechanical properties, temperature, and force generation during FSW. Proceedings of the Institution of Mechanical Engineers, Part L: Journal of Materials: Design and Applications. 2019;233(6):1033–43.
[14] Akbari M, Behnagh RA. Dissimilar friction-stir lap joining of 5083 aluminum alloy to CuZn34 brass. Metallurgical and Materials Transactions B: Process Metallurgy and Materials Processing Science. 2012;43(5):1177–86.
[15] Saravanan V, Rajakumar S, Banerjee N, Amuthakkannan R. Effect of shoulder diameter to pin diameter ratio on microstructure and mechanical properties of dissimilar friction stir welded AA2024-T6 and AA7075-T6 aluminum alloy joints. International Journal of Advanced Manufacturing Technology. 2016;87(9–12):3637–45.
[16] Kishore VR, Arun J, Padmanabhan R, Balasubramanian V. Parametric studies of dissimilar friction stir welding using computational fluid dynamics simulation. International Journal of Advanced Manufacturing Technology. 2015;80(1–4):91–8.
[17] Gerard H. Friction stir welding of dissimilar alloys for aircraft. In: 5th International Symposium on Friction Stir Welding, Metz, France, September 2004. 2004.
[18] Cole EG, Fehrenbacher A, Duffie NA, Zinn MR, Pfefferkorn FE, Ferrier NJ. Weld temperature effects during friction stir welding of dissimilar aluminum alloys 6061-t6 and 7075-t6. International Journal of Advanced Manufacturing Technology. 2014;71(1–4):643–52.
[19] Ramanjaneyulu K, Madhusudhan Reddy G, Venugopal Rao A, Markandeya R. Structure-property correlation of AA2014 friction stir welds: Role of tool pin profile. Journal of Materials Engineering and Performance. 2013;22(8):2224–40.
[20] Abd El-Hafez H, El-Megharbel A. Friction stir welding of dissimilar aluminum alloys. World Journal of Engineering and Technology. 2018;6(02):408.
[21] Waheed MA, Jaiyesimi LO, Ismail SO, Dairo OU. Analytical investigations of the effects of tool pin profile and process parameters on the peak temperature in friction stir welding. Journal of Applied and Computational Mechanics. 2017;3(2):114–24.
[22] El-Fahhar HH, Abd El-Hafez H, Ahmed MMZ, Ahmed3 E, El-Nikhaily A. The Effect of Tool Geometry on the Microstructure and Mechanical Properties of Friction Stir Processed MIG-Welded Aa5083-H111. IOSR Journal of Mechanical and Civil Engineering (IOSR-JMCE) e-ISSN. 2018;15(4):45–55.
[23] Abd El-Hafez H. Mechanical properties and welding power of friction stirred AA2024-T35 joints. Journal of materials engineering and performance. 2011;20(6):839–45.
[24] Salloomi KN, Shammari AZM, Ahmed SH. Evaluation of FSW Process Parameters of Dissimilar Aluminium Alloys. 2016;7(9).
[25] Salloomi KN. Fully coupled thermomechanical simulation of friction stir welding of aluminum 6061-T6 alloy T-joint. Journal of Manufacturing Processes. 2019;45(June):746–54.
[26] Pradeep Kumar P, Ahmmad Basha S, Sai Kumar S. Optimization of friction stir welding process

parameters of aluminium alloy AA7075-T6 by using Taguchi method. International Journal of Innovative Technology and Exploring Engineering. 2019;8(12):290–7.
[27] Abd Elnabi MM, Elshalakany AB, Abdel-Mottaleb MM, Osman TA, El Mokadem A. Influence of friction stir welding parameters on metallurgical and mechanical properties of dissimilar AA5454-AA7075 aluminum alloys. Journal of Materials Research and Technology [Internet]. 2019;8(2): 1684–93. Available from:
[28] https://doi.org/10.1016/j.jmrt.2018.10.015
[29] Li K, Jarrar F, Sheikh-Ahmad J, Ozturk F. Using coupled Eulerian Lagrangian formulation for accurate modeling of the friction stir welding process. Procedia Engineering [Internet]. 2017;207:574–9. Available from:
[30] https://doi.org/10.1016/j.proeng.2017.10.1023
[31] Amancio-Filho ST, Sheikhi S, dos Santos JF, Bolfarini C. Preliminary study on the microstructure and mechanical properties of dissimilar friction stir welds in aircraft aluminium alloys 2024-T351 and 6056-T4. Journal of materials processing technology. 2008;206(1–3):132–42.
[32] Khodir S, Shibayanagi T. Friction stir welding of dissimilar AA2024 and AA7075 aluminum alloy. Materials Science and Engineering B-advanced Functional Solid-state Materials. 2008 Feb 1;148:82–7.
[33] Guo Y, Ma Y, Wang F. Dynamic fracture properties of 2024-T3 and 7075-T6 aluminum friction stir welded joints with different welding parameters. Theoretical and Applied Fracture Mechanics. 2019;104(March).
[34] Shanmuga Sundaram N, Murugan N. Tensile behavior of dissimilar friction stir welded joints of aluminium alloys. Materials & Design. 2010;31(9):4184–93.
[35] Cavaliere P, Panella F. Effect of tool position on the fatigue properties of dissimilar 2024-7075 sheets joined by friction stir welding. Journal of Materials Processing Technology. 2008;206(1):249–55.